Gold Nanoparticles Covered Hollow SiO_2 Nanocapsules for DOX Delivery and Multiple Antitumor

CHANG guanru [1,2,a], SHEN yuhua [*1, b], PEI chun[2c] and CHEN long[2d]
[1.] No.111 Jiulong Road, Economic and Technology Development Zone, Hefei, Anhui, P.R.China
[2.] No.39 Xihai Road, Tunxi District Huangshan City, Anhui Province, P.R.China
[a] changgr@hsu.edu.cn[1], [b] s_yuhua@163.com ,[c] 18855971845@163.com,
[d] chenlong2008@hsu.edu.cn

Abstract. A chemo and photothermal therapy integrated nanoplatform, DOX-loaded and AuNPs-covered hollow SiO_2 nanocapsules (Au-HMSN@DOX), were constructed for enhanced cancer therapy via sequential NIR irradiation. HMSN are used as nanocarriers for drug delivery. AuNPs exhibit an outstanding photothermal effect for increasing the local temperature. Compared with HMSN@DOX, the combination of NIR light-triggered photothermal of AuNPs and Chemotherapy of DOX leads to enhanced antitumor effect and reduced side effect.

1. Introduction

Cancer is one of the most common causes of death and poses major threat to human health worldwide[1]. To enhance antitumor effect and minimize the side effects, nanoparticles with small sizes (90–200nm) have attracted much attention in biomedical research, which preferably accumulate at tumor sites through the enhanced permeability and retention (EPR) effect[2,3]. Therefore various nanomaterials have been widely used in cancer therapy as a carrier to deliver therapeutic agents into targeted organs or cells [4,5]. Among all the drug delivery systems, mesoporous silica nanoparticles (MSN) is readily available and most promising candidate due to their unique properties, including high surface areas, large pore volumes, tunable pore sizes and controllable surface chemistry as well as particle sizes. Especially, the hollow SiO_2 nanospheres (HMSNs) have even higher drug loading capacity, and allow the drugs to easily pass through highly porous shell [6,7].

Due to their excellent photothermal properties, Au nanoparticles (AuNPs) can absorb near-infrared light and then realize NIR photothermal ablation. AuNP-assisted photothermal treatment can be targeted with heat in each individual cell, thereby improving the controllability of hyperthermia and selective killing of tumor cells[8,9].

Herein, HMSN are chosen as drug carriers and Au nanoparticles as photothermal reagents to construct a multifunctional antitumor platform[10], which integrates chemotherapy with photothermal therapy (PTT) to offer multimodality antitumor.

* Corresponding author: changgr@hsu.edu.cn

2. Experimental Section

2.1Materials and Measurements

$HAuCl_4 \cdot 3H_2O$, $AgNO_3$, $NaBH_4$, cetyltrimethyl ammonium bromide (CTAB), L-ascorbic acid, Tetraethyoxysilane (TEOS), HCl, Doxorubicin (DOX) and polyvinylpyrrolidone (PVP, K-30) were obtained from Chemical Shanghai Reagent Co. All the chemicals were of analytical grade, and used without further purification.

SEM and TEM images were obtained on a S4800 ESEM FEG scanning electron microscope and on a JEM 2100 microscope. XRD was recorded using a DX-2700 X-Ray Diffractometer equipped with Cu Kα sealed tube (λ = 1.5406 Å). FT-IR spectra were carried out using a NEXUS-870 spectrophotometer (Thermo Fisher, USA, within 4000–500 cm^{-1}. UV-Vis absorption spectra were recorded using a UV-3900 spectrophotometer (Hitachi, Japan) over the range of 200-900 nm. IR thermal imaging was performed on IR thermal camera (Fluke, USA). The OD values of the MTT assay were recorded using a RT-2100C spectrophotometric microplate reader (Rayto, China). Fluorescence images were obtained using a DMI3000B inverted fluorescence microscope (Leica, Germany).

2.2Synthesis of Hollow Mesoporous silica Nanoparticles (HMSN)

MSNs were synthesized by the following procedures: NaOH (2 mmol/mL, 1.75 ml) was added to 240 ml of CTAB (0.504g) aqueous solution. After stirring for 15 min, 2.5ml of TEOS was added dropwise and vigorously stirred at 80℃ for 2h. The resulting nanoparticles were centrifuged, washed and calcinated at 560℃ for 6h. MSN solution (1.56 mL) is dispersed in PVP aqueous solution (8.44 mL, 3%), then 0.63 g $NaBH_4$ was added and the mixture was heated to 50℃ for 6 h. The HMSN were washed and re-dispersed in DI water at the concentration of 120 mg/mL.

2.3DOX-loading into HMSN and Au-HMSN

AuNPs were prepared by green synthesis method[10]. Au- HMSN were prepared by mixing of AuNPs solution (3.0 mL) and of HMSN solution (1.0 mL, 150 mg/mL) and the mixture is vortex vibrated and left overnight. Then the Au-HMSN was washed and re-dispersed in DI water at desired concentration for future use. For the loading of DOX, HMSNs or Au-HMSN (6 mg) were dispersed into DOX aqueous solution (6 mL, 0.5 mg/mL). After dispersion and stirring under light-sealed conditions for 12 h, the obtained samples were centrifuged and washed, then re-dispersed in DI water.

2.4Controlled Release Experiments

For examining the photothermal effect of Au-HMSN, the samples (100m L, 2.0 mg/mL) are exposed to NIR laser light (808 nm, 200 mW/cm^2) for 15 min, IR thermal imaging was used to monitor the temperature. In order to evaluate the DOX release profiles of the Au-HMSN in the PBS buffer solutions (pH 5.0) , the sample solution (121 mg/mL) was vortex vibrated for 20 min, and then centrifuged at 8000 rpm for 10 min. The content of DOX in the supernatant is derived by measuring the UV-vis absorption at 588 nm.

2.5Cytotoxicity Assay and Fluorescence Image

Cell viability was determined using a MTT assay [11]. HeLa cells were seeded (5×10^3/well) into 96-well plates and incubated for 24 h. Different concentrations of samples in medium solution (5, 10, 50μg /mL) were added to the cells and irradiated for 10 min. Following incubation for 24 h, the MTT solution (20 μL, 5mg/mL) was added and further cultured for 4 h before DMSO (150 μL) was added. The absorbance at 490 nm was measured using a spectrophotometric microplate reader, and cellular survival rates were calculated according to the OD values.

For fluorescence microscope imaging, Hela cells were seeded in 6-well plates, and after incubated for 24 h, 3 mL of fresh DMEM medium containing 50μg samples were added. After incubated for 6 h, the plate was subjected to 660 nm laser light for 10 min, then were successively stained with 0.5 mL of Hoechst 33342 and PI (1 μg/mL) for 20 min in the darkness. Dual fluorescence-stained cells were washed with PBS and observed under an inverted fluorescence microscope. All experiments were carried out in triplicate.

3. Results and Discussion

MSN are prepared by TEOS hydrolysis based on the Stöber process with a little medication and Au nanoparticles are obtained via bioreduction method . SEM images of the HMSN, DOX-loaded HMSM, AuNPs and Au-HMSN are presented in Fig. 1.

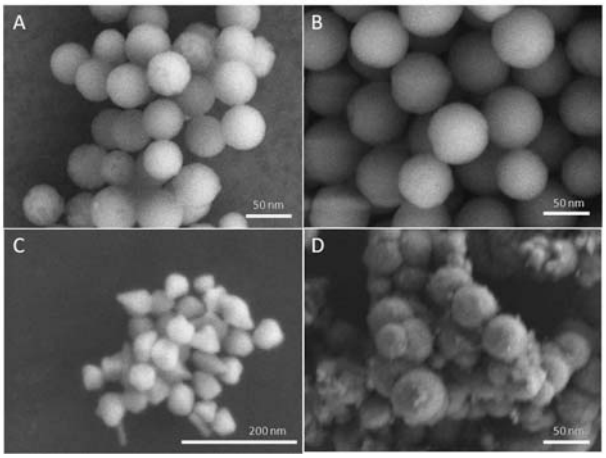

Fig. 1 SEM images of (A) HMSN, (B) HMSN@DOX,(C) AuNPs, (D) Au-HMSN

As shown in Fig. 1A and B, HMSN, HMSN@DOX both exhibited a highly uniform and monodispersed spherical morphology about 100 nm in size. Compared with HMSN, the surface of HMSN@DOX was smooth. Most of Au nanoparticals in Fig.1C possess spherer shape with diameters of 20 nm. HMSN are obtained by a selective etching strategy. In the etching process, PVP is added to prevent aggregation of HMSN and serves as a bridging agent between the hollow SiO_2 and Au NPs. Fig.1D presents a typical SEM image of AuNPs covered HMSN (Au-HMSN) and the AuNPs outside the mesoporous silica shell are randomly distributed.

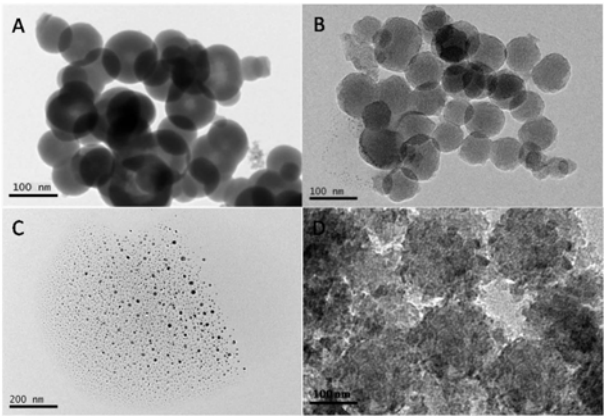

Fig. 2 TEM images of (A) HMSN, (B) MSN@DOX,(C) AuNPs, (D) Au-HMSN.

As shown in Fig. 2A, TEM images of the HMSN illustrate well-defined hollow nanostructures with discernable pores on the surface, which allow DOX to pass through and load onto the SiO_2 shells. The spheres are about 100 nm in size and the internal diameter 30 nm. TEM image (Fig. 1c) shows that DOX were encapsulated inside the hollow silica nanospheres . The corresponding TEM images further confirmed that the hollow nature of the spheres and the random uniform distribution of Au NPs mainly on the surface of MSNCs.

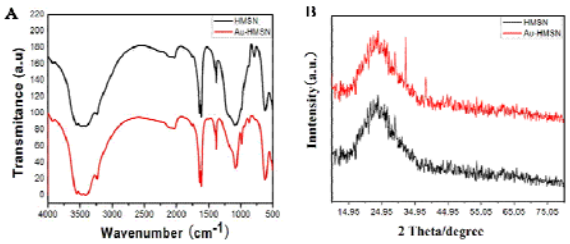

Fig. 3. FT-IR spectra and XRD patterns of HMSN and HMSN-Au

FT-IR spectra for HMSN before and after Au nanoparticals covered are shown in Fig. 3A. After etching by $NaBH_4$ in PVP solution, the MSN exhibit an obvious solid-to-hollow structure conversion. Compared with the FTIR spectrum of MSN, a red shift is observed within the broad absorption region of 1088 cm^{-1}, which is assigned to the Si –O – Si asymmetric stretching vibration. This absorption makes the Si– OH stretching vibration band at 982 cm^{-1} unobservable due to overlap. In addition, the Si– O – Si symmetric stretching vibration at 806 cm^{-1} shifts to 788 cm^{-1}.These shifts are attributed to a more open SiO_2 network structure. We also could conclude from the comparison of Fig.3A and B that the existence of AuNPs has no major impact on the FTIR spectra. XRD patterns of the HMSN and Au-HMSN hybrids are shown in Fig. 2B. As shown in curve a, the broad amorphous peak is observed at 24.95°, which is attributed to HMSN sample. And the diffraction peak at 2θ value of 38.2° is indexed to be (111) plan of AuNPs (JCPDS No.4-0784). The results confirm the presence of AuNPs outside of the hollow SiO_2 nanocapsules.

Due to the high surface-volume ratio, and electron-phonon coupling, AuNPs usually can serve as a photothermal antineoplastic material, also prevent the leakage of DOX from the hollow structure. Fig. 4A shows the IR thermal images of H_2O and Au-HMSN solution when exposed to the NIR laser (808 nm, 300mW·cm^{-2}) for 10 min, temperature increments

of Au-HMSN is 14.5℃, whereas the water temperature increased by only 4.8 ℃ under the same conditions.

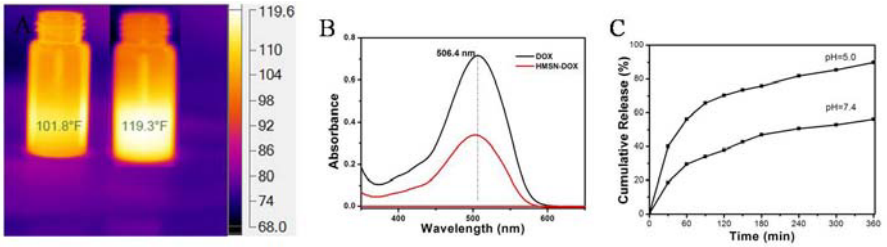

Fig. 4 Thermal infrared images (A) of Au-HMSN under NIR (808 nm, 300 mW) irradiation for 15 min; UV spectra (B) of the DOX solution before and after loaded in the Au-HMSNs In vitro drug release(C) from Au-HMSNs at pH 5.0 before and after NIR irradiation

The absorption spectra of DOX before and after loading were shown in Fig. 4B. The decrease of DOX concentration in the supernatant demonstrates the storage into the cavities and pores of HMSN. PBS solution at pH 5.0 was used to simulate the intracellular conditions of HeLa cells. The in vitro release of DOX from Au-HMSN before and after NIR irradiation were examined in PBS (pH 5.0) at 37 °C. Fig. C shows that Au- HMSNs could release DOX in a temperature-dependent controlled release manner, and the drug release rate was much faster under irradiation. Therefore, the continuous release of DOX can be regulated by manipulating the NIR irradiation.

The standard MTT assay was conducted to determine the relative viability of HeLa cells incubated with different concentrations of samples, and their relative survival rates are shown in Fig 5.

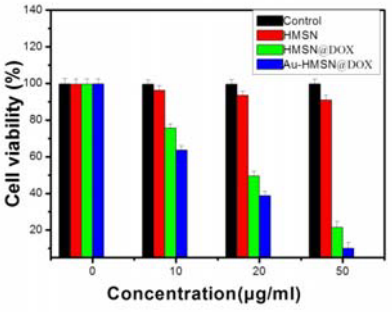

Fig.5 Viability of Hela cells (control) and incubated with different concentrations of HMSN, HMSN@DOX and Au-HMSN@DOX under irradiation.

As expected, the cell survival rates of samples in Fig.5 exhibited a downward trend when the concentrations of HMSN@DOX and Au-HMSN@DOX increase under irradiation. However, similar dose-dependent cytotoxicity behavior was not observed in case of HeLa cells incubated with HMSN. The results indicate that HMSN are biocompatible and excellent carriers, and the loading of DOX brings about obvious cytotoxicity. After 10 min of sequential NIR irradiation, the relative viabilities of Hela cells treated by HMSN@DOX and Au-HMSN@DOX at the concentration of 50μg/mL sharply decrease to 21.4% and10.1%. The results reveal that both chemotherapeutics loaded inside of HMSN and AuNPs covered outside give rise to remarkably anticancer efficiency,

Au-HMSN@DOX can serve as a potential high-performance platform for synergistic antitumor.

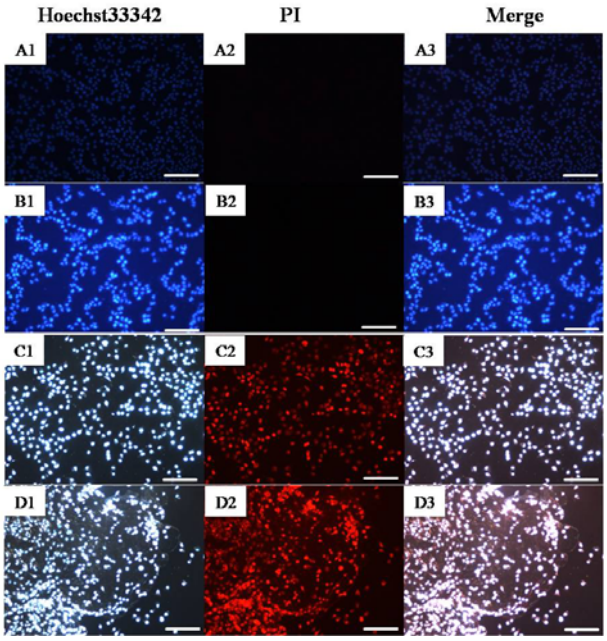

Fig.6 Fluorescence microscopy images of Hela cells as a control without (A) and with irradiation (B), and Hela cells incubated with (C) HMSN@DOX and(D) Au-HMSN@DOX under irradiation; Hela cell as a control (1), dyed by Hoechst 33342 (2), red by PI (3) and the merged images of both above (4); The scale bar is 200 μm.

The antitumor effects of the HMSN@DOX and Au-HMSN@DOX were further investigated by fluorescence microscope with PI/Hoechst 33342 double staining. And fluorescence images of HeLa cells under different conditions are shown in Fig. 6. Hoechst 33342 can freely pass through cell membranes and stain nuclear DNA in blue, while PI only enters necrotic cells or late-phase apoptotic cells to stain nuclear DNA in red [12]. As a control group (Fig. 6A and 6B), Hela cells grow exuberantly before or even after laser irradiation, without their nuclei appearing red. Fig. 6C and 6D show cells incubated with HMSN@DOX and Au-HMSN@DOX with NIR irradiation for 10min, respectively, strong red fluorescence images and purple merged images can be observed. Such a fact demonstrates HeLa cells are effectively killed by chemo and photothermal therapy due to the presence of DOX and Au nanoparticals, which is in agreement with the MTT results.

4. Conclusion

We fabricated DOX-loaded and AuNPs-covered hollow SiO_2 nanocapsules (Au-HMSN@DOX). The hybrid nanomaterial could serve as chemo and photothermal therapy integrated platform for enhanced cancer therapy via sequential irradiation as stimuli. AuNRs exhibit an outstanding photothermal effect for increasing the local temperature in lesions and the therapeutic effect of the Au-HMSN@DOX has significantly improved compared with HMSN@DOX. This demonstrates a synergistic antitumor effect between each component of the hybrid Au-HMSN@DOX, which would reduce the dosage and the side effect of the DOX.

5. Acknowledgment

This work is supported by Key project of the natural science foundation of the provincial education department(KJ2016A679), Key projects of university excellent talent support program (gxyqZD2016302), Provincial college students' scientific research innovation projects(201510375048，AH201310375053)； Scientific research project of Huangshan college (2006xkjq007)

References

1. A. Umar, B.K.Dunn, P. Greenwald, submitted to Nat.Rev Cancer (2012).
2. S. Wu，X. Huang，X. Du, submitted to Angewandte Chemie International Edition(2013)
3. M.H. Yu, S. Jambhrunkar, P.Thorn, J.Z. Chen, W.Y. Gu, C.Z. Yu, submitted to Nanoscale (2013).
4. R.A. Petros,J.M. DeSimone, submitted to Nat Rev Drug Discov (2010)
5. J.Shen, G.S. Song, M. An, X.Q. Li, N. Wu, et al, submitted to *Biomaterials (*2014*)*
6. T. Wang, F. Chai, Q. Fu, L. Zhang, H. Liu, L. Li, et al, submitted to J Mater Chem (2011)
7. L. Li, F. Tang, H. Liu, T. Liu, N. Hao, D. Chen, et al. et al, submitted to ACS Nano (2010)
8. B. Hu, L. P. Zhang, X.W.Chen, J.H.Wang, Nanoscale (2013).
9. A. Ulatowska-Jar.za, J. Zychowicz, I. Holowacz, J. Bauer, J. Razik, A. Wieliczko, et al, submitted to Med. Laser. Appl. (2006)
10. S. Shen, H. Tang, X. Zhang, J. Ren, Z. Pang, D. Wang, et al, submitted to Biomaterials (2013).
11. B. Kundu, S.C. submitted to Biomaterials (2012).
12. J. Zhao, Y. Huang, Y. Song, X. Zhao, J. Jin, J. Wang, et al, submitted to Toxicol. Lett. (2009).